Cyclic Peptidomimetics Derived from the Apical Membrane Antigen I of *Plasmodium falciparum* and Their Use in Malaria Vaccine Design

by **Annabelle Renard**[a]), **Markus Mueller**[b]), **Rinaldo Zurbriggen**[c]), **Gerd Pluschke**[b]), and **John A. Robinson***[a])

[a]) Institute of Organic Chemistry, University of Zürich, Winterthurerstrasse 190, CH-8057 Zürich (phone: +41-1-635-4242; fax: +41-1-635-6833; e-mail: robinson@oci.unizh.ch)
[b]) Molecular Immunology, Swiss Tropical Institute, CH-4002 Basel
[c]) Pevion Biotech, CH-3018, Bern

Dedicated to Professor *Duilio Arigoni* on the occasion of his 75th birthday

A library of 35 cyclic peptidomimetics has been prepared, by a combination of solid- and solution-phase methods, which, together, scan amino acid residues 444–489 in a protruding loop in the subdomain-III of the apical membrane antigen-I (AMA-I), an integral membrane protein found on the surface of *Plasmodium falciparum* merozoites. The mimetics each contain twelve residues from AMA-I linked through the N- and C-termini to a β-hairpin-inducing template, comprising the dipeptide D-proline-L-Apro (Apro = *cis*-4-amino-L-proline). These peptidomimetics were each coupled *via* the 4-amino group to a phospholipid, which allows their incorporation into reconstituted influenza virus-like particles (virosomes) for immunization of mice, as well as their use in ELISA to characterize epitopes recognized by anti-AMA-I growth-inhibitory monoclonal antibodies.

1. Introduction. – Cyclic-peptide mimetics offer several potential advantages over linear peptides as antigens and immunogens in synthetic vaccine design [1–3]. For example, in a cyclic mimetic, biologically relevant conformations may be stabilized, and proteolytic stability in serum may be significantly enhanced compared to a linear peptide. Cyclic epitope mimetics may be used as immunogens to elicit antibodies that cross-react with a target protein, and be useful as antigens for characterizing epitopes recognized by inhibitory antibodies.

An important issue in using peptidomimetics as immunogens is the way in which they are delivered to the immune system. Small molecules are usually first coupled to a carrier protein, and the conjugates are then injected together with an immunostimulatory adjuvant to elicit immune responses in animals. On the other hand, the use of reconstituted influenza virosomes as an alternative delivery vehicle to induce humoral immune responses against peptides and peptidomimetics has been demonstrated recently [2][4][5]. Virosomes are reconstituted virus-like particles, incorporating the influenza virus hemagglutinin and neuraminidase membrane glycoproteins, but lacking nucleic acids in their interior. By linking the peptide or mimetic of interest to a phospholipid, it may be anchored in the membrane and be exposed on the virosome surface in a native-like conformation, and in a highly immunogenic format. The fusogenic properties of the hemagglutinin may facilitate uptake of the virosome by immunocompetent cells and entry of the mimetics into the natural antigen-processing pathways [6][7]. Furthermore, virosomes have been licensed already for human

clinical use, in the form of vaccines against influenza (*Inflexal*™) and hepatitis A (*Epaxal*™) [8][9], which may facilitate testing new virosome-based peptidomimetic vaccine candidates in humans.

We describe here the synthesis of epitope mimetics of the apical membrane antigen I (AMA-I) of the most serious human malaria parasite *Plasmodium falciparum*. AMA-I is an asexual blood-stage protein expressed in the invasive merozoite form of *Plasmodia* species. It plays a key role in the invasion of red blood cells [10], and is a leading candidate antigen for inclusion as a recombinant protein in a malaria-subunit vaccine [11][12]. It is a type-1 integral membrane protein with one transmembrane domain and an ectodomain that can be divided into three subdomains, each with structures stabilized by multiple disulfide bonds [13]. The three-dimensional NMR solution structure of subdomain-III in AMA-$1^{436–545}$ was recently shown to adopt a cysteine-knot-like motif (*Figs. 1* and *2*) [14]. In this work, we focus on one surface loop AMA-$I^{444–489}$ located between the first two cysteines (Cys^{443} and Cys^{490}) in subdomain-III. It was demonstrated recently that a virosomal formulation of a synthetic epitope mimetic comprising residues 446–490 of AMA-I elicits parasite-specific and growth-inhibitory antibodies in mice [15]. This construct is of interest in the design of a synthetic malaria-vaccine candidate, targeting the erythrocytic stage of *P. falciparum*.

Here, we set out to construct a library of smaller cyclic peptidomimetics:

- each containing only twelve residues derived from AMA-$I^{444–489}$
- which together scan $AMA^{444–489}$ with sequential library members displaced along the primary sequence by one amino acid
- each being template-bound to stabilize potential β-hairpin conformational epitopes
- each being attached to a phospholipid to facilitate incorporation into virosomes, and for use in ELISA (enzyme-linked immunosorbent assay).

We describe below the design and synthesis of this library and its use to characterize anti-AMA-I growth-inhibitory monoclonal antibodies.

2. Results and Discussion. – 2.1. *Library Design*. One of the goals of this work was to identify mimetics of putative β-hairpin structures in the AMA-I domain III to be used both to elicit antibodies cross-reactive with the native AMA-I protein and to map epitopes recognized by parasite-specific, growth-inhibitory antibodies.

Residues AMA-$I^{444–489}$ constitute a large surface loop between the first and second cysteines (Cys^{443} and Cys^{490}) within the cysteine-knot-like motif in subdomain-III (*Figs. 1* and *2*) [13][14]. The cysteine-knot motif derives its name from the common, tightly-packed core found in many growth factors whose folded structures are stabilized by three conserved disulfide bridges [16]. Other examples of known 3D structure include platelet-derived growth factor (PDGF), vascular endothelial growth factor (VEGF), and nerve growth factor (NGF) [17]. The loop between cysteines-1 and -2 in these proteins typically contains one (*e.g.*, PDGF) or several (*e.g.*, NGF) individual β-hairpin motif(s). Hence, we surmised that β-hairpin motifs might also be present in the corresponding region of native full-length AMA-I. In the published NMR solution structure of AMA-$1^{436–545}$ (PDB file 1 HN6), this loop region is structurally disordered (see *Fig. 1*) [14]. However, it seems reasonable that a folded structure for this region should be expected in the native full-length ectodomain, *e.g.*, stabilized through

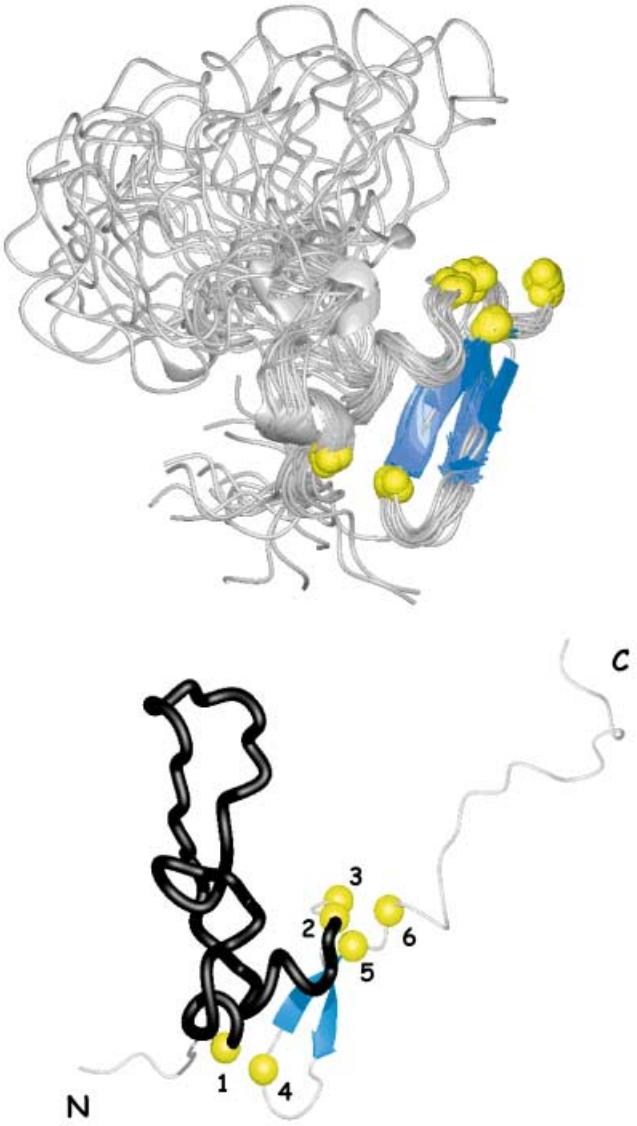

Fig. 1. *Ribbon diagram of subdomain-III from AMA-I* (prepared from PDB file 1HN6), *which includes residues 436–545*. Above: overlay of residues 436–509 in 20 best-fit NMR structures. Below: the black cylinder represents residues 444–489 in one NMR structure. The positions (C(α)-atoms) of the six cysteine residues (numbered 1–6 in sequence) in subdomain-III are represented by yellow balls. The N and C termini are marked.

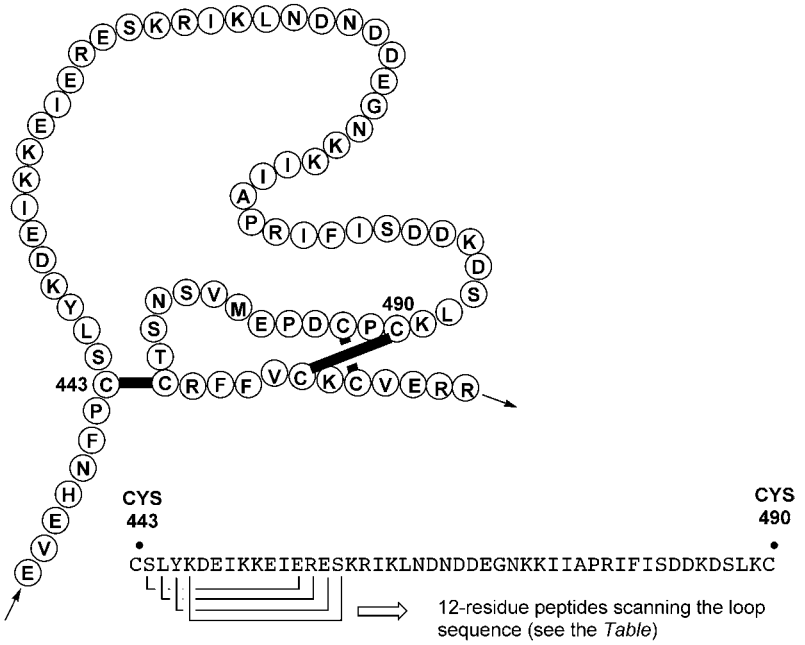

Fig. 2. *The primary sequence of AMA-I domain-III.* The loop lying between residues 443 – 490 is highlighted along with some of the twelve-residue segments that have been transplanted onto the hairpin-inducing ^{D}Pro-Apro template (see *Fig. 3*).

interactions with other (sub)domains of AMA-I or other proteins on the surface of the parasite.

For this work, we chose to prepare a library of twelve-residue peptidomimetics to scan this large loop (*Fig. 2*), each mounted on a β-hairpin-inducing template, and each displaced by one residue in sequence relative to the next, so that any β-hairpin structure present in the native AMA-I$^{444–489}$ loop has a chance to be mimicked in one of the library members. As a hairpin-inducing template, we focused initially on the dipeptide ^{D}Pro-^{L}Pro, which has already been used to prepare β-hairpin mimetics derived from PDGF [18], from antibody hypervariable loops (CDRs) [19], a protease inhibitor [20], and mimics of cationic antimicrobial peptides [21]. However, so that each library member can be conjugated with a phospholipid, the ^{L}Pro residue in the template was replaced by (2*S*,4*R*)-4-aminoproline (Apro) (*Fig. 3*) [22]. The 4-NH_2 group in Apro can then be used to link each mimetic to a phospholipid. The targets for synthesis were, therefore, the library of 35 mimetics represented by the general formula **1** (*Fig. 3*), having the twelve-mer loop sequences shown in the *Table* (*cf.* also *Fig. 2*).

2.2. *Synthesis.* We already described the use of Fmoc-Apro(Ddiv)-OH[1]) for the synthesis of β-hairpin mimetics [22], where the 4-amino group was protected with the Ddiv-group [23]. Here we chose to use an orthogonally protected Fmoc-Apro(Alloc)-OH derivative. Fmoc-Apro(Alloc)-OH (**5**) was readily accessible from (2*S*,4*S*)-4-

[1]) For abbreviations, see the *Exper. Part.*

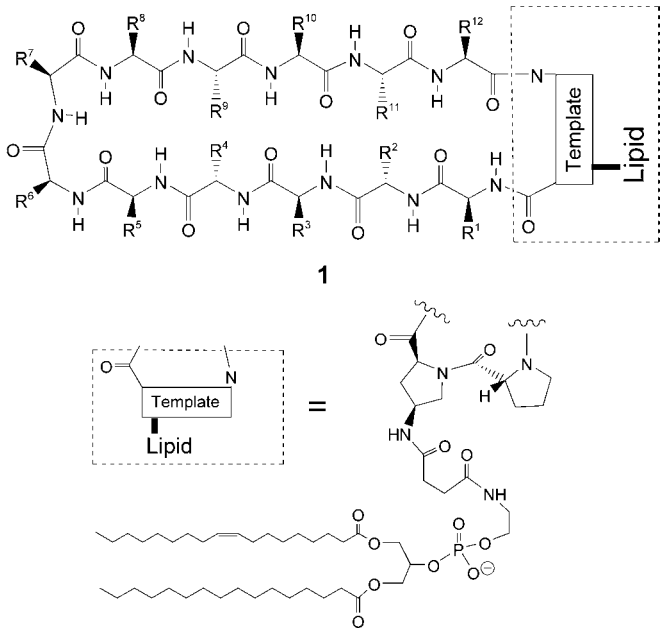

Fig. 3. *Constitution of the synthesized peptidomimetics.* [D]Pro-Apro template is coupled *via* a succinate linker to the phospholipid. The sequences of the 35 peptidomimetics that scan the 444 – 489 region in AMA-I domain-III are shown in the *Table*.

hydroxyproline, as outlined in *Scheme 1*. This route is closely related to published procedures (see, *e.g.*, [24]).

Scheme 1

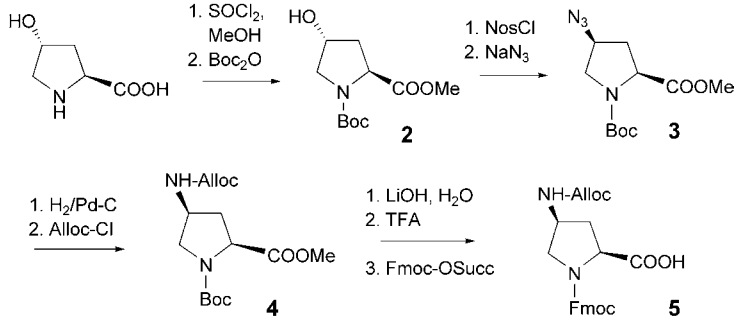

Alloc = Allyloxycarbonyl (= (prop-2-enyloxy)carbonyl), Fmoc = [(9*H*-fluoren-9-yl)methoxy]carbonyl, Nos = (4-nitrophenyl)sulfonyl, Succ = succinyl, TFA = 2,2,2-trifluoroacetic acid.

The synthetic route to the library of peptidomimetics (*Scheme 2*), involves first the assembly of the resin-bound linear precursor **6** by means of Fmoc solid-phase peptide chemistry [25]. Typically, the synthesis of each mimetic was started from the sixth residue within the twelve-mer sequence, and the macrocyclization was performed in

Table. *Data of 35 Cyclic Hairpin Mimetics, Each Containing Twelve Residues from the AMA-I*$^{444-489}$ *Loop* (for structures, *cf. Fig. 3*).

Entry	Residues	Sequence	Formula	M_w (calc.)	m/z [a])
1	444–455	SLYKDEIKKEIE	$C_{120}H_{202}N_{19}O_{34}P$	2486.0	1244.2 ([$M+2$H])
2	445–456	LYKDEIKKEIER	$C_{123}H_{209}N_{22}O_{33}P$	2555.1	1279.1 ([$M+2$H]), 852.1 ([$M+3$H])
3	446–457	YKDEIKKEIERE	$C_{122}H_{205}N_{22}O_{35}P$	2571.1	1286.4 ([$M+2$H]), 858.1 ([$M+3$H])
4	447–458	KDEIKKEIERES	$C_{116}H_{201}N_{22}O_{35}P$	2495.0	832.7 ([$M+3$H]), 624.9 ([$M+4$H])
5	448–459	DEIKKEIERESK	$C_{116}H_{201}N_{22}O_{35}P$	2495.0	832.8 ([$M+3$H])
6	449–460	EIKKEIERESKR	$C_{118}H_{208}N_{25}O_{33}P$	2536.1	1268.7 ([$M+2$H]), 846.3 ([$M+3$H]), 635.0 ([$M+4$H])
7	450–461	IKKEIERESKRI	$C_{119}H_{212}N_{25}O_{31}P$	2520.1	1261.2 ([$M+2$H]), 841.2 ([$M+3$H])
8	451–462	KKEIERESKRIK	$C_{119}H_{213}N_{26}O_{31}P$	2535.2	635.0 ([$M+4$H])
9	452–463	KEIERESKRIKL	$C_{119}H_{212}N_{25}O_{31}P$	2520.1	1260.7 ([$M+2$H]), 841.0 ([$M+3$H]), 631.0 ([$M+4$H])
10	453–464	EIERESKRIKLN	$C_{117}H_{206}N_{25}O_{32}P$	2506.0	1253.7 ([$M+2$H]), 836.3 ([$M+3$H])
11	454–465	IERESKRIKLND	$C_{116}H_{204}N_{25}O_{32}P$	2492.1	1247.4 ([$M+2$H]), 831.3 ([$M+3$H])
12	455–466	ERESKRIKLNDN	$C_{114}H_{199}N_{26}O_{33}P$	2493.0	1247.0 ([$M+2$H]), 831.9 ([$M+3$H])
13	456–467	RESKRIKLNDND	$C_{113}H_{197}N_{26}O_{33}P$	2478.9	2479.7 ([$M+$H]), 1240.2 ([$M+2$H]), 827.5 ([$M+3$H])
14	457–468	ESKRIKLNDNDD	$C_{111}H_{190}N_{23}O_{35}P$	2437.9	2438.8 ([$M+$H]), 1220.3 ([$M+2$H])
15	458–469	SKRIKLNDNDDE	$C_{111}H_{190}N_{23}O_{35}P$	2437.9	1219.9 ([$M+2$H]), 813.4 ([$M+3$H])
16	459–470	KRIKLNDNDDEG	$C_{110}H_{188}N_{23}O_{34}P$	2407.8	2409.6 ([$M+$H]), 1205.4 ([$M+2$H])
17	460–471	RIKLNDNDDEGN	$C_{108}H_{182}N_{23}O_{35}P$	2393.8	2394.9 ([$M+$H]), 1198.0 ([$M+2$H])
18	461–472	IKLNDNDDEGNK	$C_{108}H_{182}N_{21}O_{35}P$	2365.8	1183.4 ([$M+2$H]), 789.3 ([$M+3$H])
19	462–473	KLNDNDDEGNKK	$C_{108}H_{183}N_{22}O_{35}P$	2380.8	2382.9 ([$M+$H]), 1191.3 ([$M+2$H])
20	463–474	LNDNDDEGNKKI	$C_{108}H_{182}N_{21}O_{35}P$	2365.8	2367.0 ([$M+$H]), 1183.9 ([$M+2$H])
21	464–475	NDNDDEGNKKII	$C_{108}H_{182}N_{21}O_{35}P$	2365.8	2366.1 ([$M+$H]), 1183.9 ([$M+2$H])
22	465–476	DNDDEGNKKIIA	$C_{107}H_{181}N_{20}O_{34}P$	2322.7	2324.6 ([$M+$H]), 1162.8 ([$M+2$H])
23	466–477	NDDEGNKKIIAP	$C_{108}H_{183}N_{20}O_{32}P$	2304.8	2306.8 ([$M+$H]), 1153.1 ([$M+2$H])
24	467–478	DDEGNKKIIAPR	$C_{110}H_{189}N_{22}O_{31}P$	2346.8	1174.2 ([$M+2$H]), 783.4 ([$M+3$H])
25	468–479	DEGNKKIIAPRI	$C_{112}H_{195}N_{22}O_{29}P$	2344.9	2345.2 ([$M+$H]), 1173.1 ([$M+2$H]), 782.6 ([$M+3$H])
26	469–480	EGNKKIIAPRIF	$C_{117}H_{199}N_{22}O_{27}P$	2377.0	2377.5 ([$M+$H]), 1189.4 ([$M+2$H])
27	470–481	GNKKIIAPRIFI	$C_{118}H_{203}N_{22}O_{25}P$	2361.1	2361.4 ([$M+$H])
28	471–482	NKKIIAPRIFIS	$C_{119}H_{205}N_{22}O_{26}P$	2391.1	1196.5 ([$M+2$H])
29	472–483	KKIIAPRIFISD	$C_{119}H_{204}N_{21}O_{27}P$	2392.0	2391.3 ([$M+$H]), 1196.0 ([$M+2$H])
30	473–484	KIIAPRIFISDD	$C_{117}H_{197}N_{20}O_{29}P$	2379.0	2379.3 ([$M+$H]), 1190.3 ([$M+2$H])
31	474–485	IIAPRIFISDDK	$C_{117}H_{197}N_{20}O_{29}P$	2379.0	2379.0 ([$M+$H]), 1190.0 ([$M+2$H])
32	475–486	IAPRIFISDDKD	$C_{115}H_{193}N_{20}O_{31}P$	2380.9	1191.2 ([$M+2$H])
33	476–487	APRIFISDDKDS	$C_{112}H_{185}N_{20}O_{32}P$	2354.8	2355.9 ([$M+$H]), 1178.9 ([$M+2$H])
34	477–488	PRIFISDDKDSL	$C_{115}H_{191}N_{20}O_{32}P$	2396.9	1199.9 ([$M+2$H])
35	478–489	RIFISDDKDSLK	$C_{116}H_{196}N_{21}O_{32}P$	2427.9	1215.1 ([$M+2$H]), 810.0 ([$M+3$H])

[a]) Electrospray-ionization (ESI) mass spectra were recorded on a *Finnigan TSQ-700* spectrometer (accuracy: ±0.1%).

solution by coupling between the sixth and seventh residues, *i.e.*, the first and last residues to be incorporated, respectively. It is not essential that the macrocycle is closed between the sixth and seventh residues, but placing the template near the center of the linear sequence may favor cyclization. The quality of each linear peptide made in this way was checked by reversed-phase HPLC after cleavage from a small portion of the resin with 1% TFA in CH_2Cl_2. The linear intermediates were typically ≥80% homogeneous, consistent with their mostly problem-free assembly.

Scheme 2. *Solid-Phase Peptide Synthesis* (SPPS) *of the Functionalized Cyclopeptides* **8**. For abbreviations, see the *Exper. Part* and *Scheme 1*.

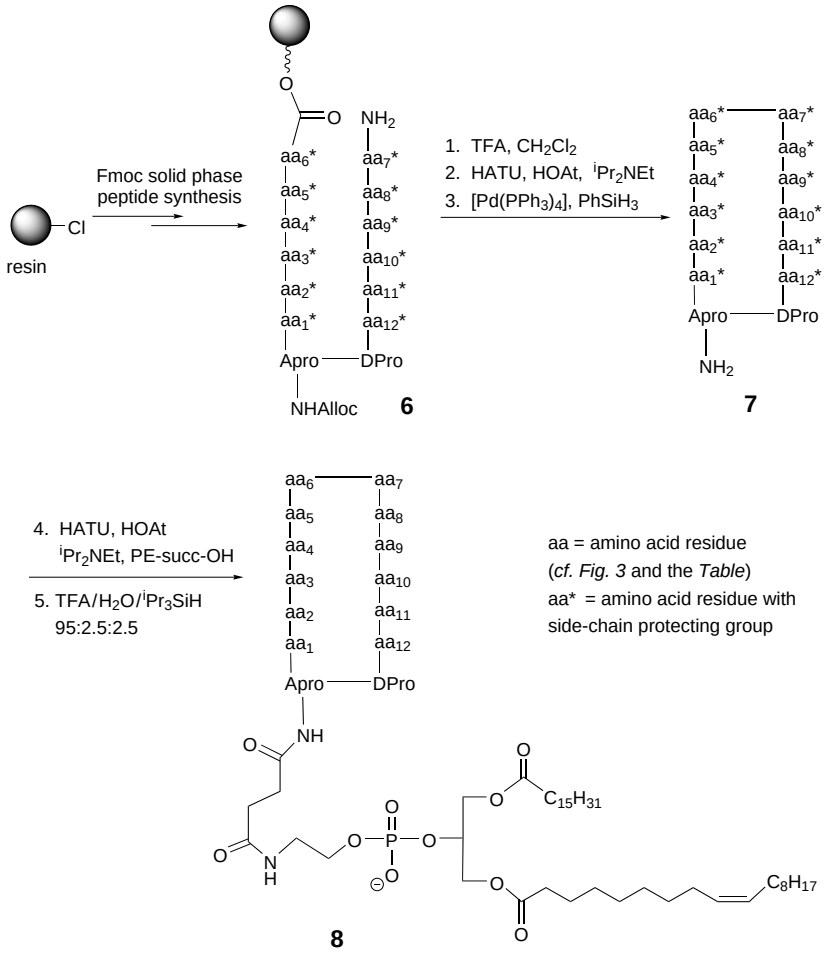

The resin-bound linear precursor **6** was then cleaved from the resin with 1% TFA/CH_2Cl_2, and macrocyclization was performed in DMF solution at a concentration of *ca.* 2 mg/ml. The quality of each macrocyclic product was assessed by HPLC and mass spectrometry (MS) after removing the Alloc-protecting group (*cf. Scheme 2*). In the majority of cases, the intermediates **7** required purification at this stage by preparative HPLC to afford materials of $\geq 90\%$ homogeneity. All the intermediates gave the expected molecular ions detected by electrospray-ionization (ESI) MS.

The phospholipid (PE-succ-OH), containing a regioisomer of phosphatidylethanolamine (PE), prepared as shown in *Scheme 3* from racemic 1-palmitoyl-3-oleoyl-*glycero*-2-phosphoethanolamine (**9**), was then coupled to the free NH_2 group of **7**. In the final step, removal of all side-chain protecting groups with 95% TFA gave the

products **8**, which were purified by HPLC on a C_4 HPLC column. ESI-MS of each product confirmed the expected masses (*cf.* the *Table*).

The formation of a side product was observed in the final deprotection step during the production of each mimetic, which could be separated by HPLC. They showed a mass 114 units higher than expected. We suspect that they arise through addition of TFA to the C=C bond in the oleoyl chain of the phospholipid. This addition reaction was observed upon treatment of PE-succ-OH with TFA under similar conditions. Subsequent work (data not given) showed that this problem can be avoided by coupling the peptidomimetic to a phospholipid containing *two* palmitoyl chains, *i.e.*, 1,3-dipalmitoyl-*glycero*-2-phosphoethanolamine, which also has the advantage of being achiral.

Scheme 3

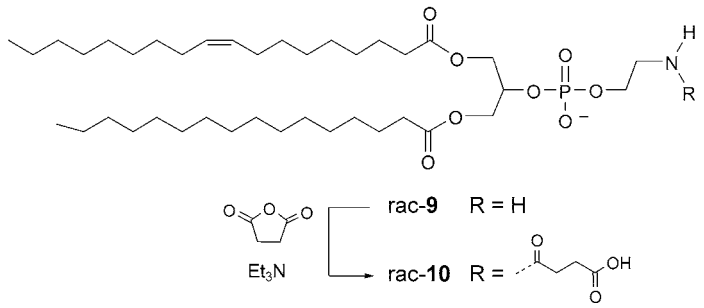

2.3 *Immunochemistry.* To determine whether any of the 35 mimetics (*Entries 1–35*, *Table*) could elicit AMA-I- and parasite-specific antibodies, each was incorporated into virosomes and used to immunize BALB/c mice. The results of this study are described in detail elsewhere [15]. Briefly, whereas all 35 mimetics elicited significant antibody titers against the respective immunizing molecule, only serum samples raised against AMA$^{458–469}$ and AMA$^{464–475}$ were weakly cross-reactive with blood-stage parasites in an immunofluorescence assay. The other mimetics elicited no significant anti-AMA-I antibodies. It seems, therefore, that parasite-cross-reactive epitopes are not accurately represented within this library of mimetics. It is interesting that a larger AMA-I$^{446–490}$ linear peptide is able to efficiently elicit growth-inhibitory antibodies [15], although several lines of evidence suggest that the correct conformation of the AMA-I protein is critical for its use as a vaccine. Although poor results were obtained here with the twelve-mer mimetics, it remains to be seen whether different, perhaps larger, cyclic forms may generate improved immune responses.

The library of mimetics has also been used as antigens in ELISA to characterize epitopes recognized by parasite-binding growth-inhibitory antibodies raised against the larger AMA-I$^{446–490}$ immunogen [15]. The phospholipid moiety facilitates immobilization of the mimetics on an ELISA plate such that the peptide is still accessible for antibody binding. For example, the inhibitory monoclonal antibody DV5 was shown by ELISA to bind selectively to the twelve-mer mimetics *10–16* (*Table*), suggesting that the epitope bound by this antibody may be at least partially represented by the core residues K^{459}RIKLN^{464}. Although the AMA-I$^{446–490}$ mimetic, in both linear and cyclized

versions, elicits high titers of inhibitory antibodies in mice, it would nevertheless be valuable to identify a smaller molecule with a similar immunogenicity. The epitope mapping studies may prove helpful in the design of new, second-generation AMA-I epitope mimetics as potential malaria vaccine candidates.

This work was supported by grants from the *Swiss Commission for Technology and Innovation*, and from the *World Health Organization* through the UNDP/World Bank/WHO special program for research and training in tropical diseases.

Experimental Part

Abbreviations. Alloc, allyloxycarbonyl (=(prop-2-enyloxy)carbonyl); Boc, (*tert*-butoxy)carbonyl; Ddiv, '1-(4,4-dimethyl-2,6-dioxocyclohexylidene)isovaleryl' (=2,2-dimethyl-5-(3-methylbutanoyl)cyclohexane-1,3-dione); Fmoc, [(9*H*-fluorenyl)methoxy]carbonyl; DMF, *N*,*N*-dimethylformamide; HATU, 2-(1*H*-7-azabenzotriazole-1-yl)-1,1,3,3-tetramethyluronium hexafluorophosphate; HBTU, 2-[1*H*-benzotriazol-1-yl]-1,1,3,3-tetramethyluronium hexafluorophosphate; HOAt, 1-hydroxy-7-azabenzotriazole (=3*H*-[1,2,3]triazolo[4,5-*b*]pyridin-3-ol); HOBt, 1-hydroxybenzotriazole (=1*H*-1,2,3-benzotriazol-1-ol); NMP, 1-methyl-2-pyrrolidone; Pbf, dihydro-2,2,4,6,7-pentamethyl-2,3-benzofuran-5-sulfonyl; TFA, trifluoroacetic acid; TIPS, triisopropylsilane; Trt, trityl (=triphenylmethyl).

Peptide Assembly. Peptide synthesis was performed on an *ABI-433A* peptide synthesiser (*Applied Biosystems*) by means of solid-phase Fmoc chemistry. The following protected Fmoc amino acid derivatives were used: Fmoc-Asn(Trt)-OH, Fmoc-Asp(^{t}Bu)-OH, Fmoc-Arg(Pbf)-OH, Fmoc-Glu(^{t}Bu)-OH, Fmoc-Lys(Boc)-OH, Fmoc-Ser(^{t}Bu)-OH, and Fmoc-Tyr(^{t}Bu)-OH. Peptides were synthesized on 2-chlorotrityl chloride resin (*ca.* 200 mg resin; average loading 0.5 mmol/g). Coupling reactions were performed with 1 mmol of each amino acid, activated *in situ* with HBTU and HOBt in DMF (0.45M), and iPr_2NEt in NMP (2M).

Cleavage from the Resin, Cyclization, and Alloc-Deprotection. After assembly, the linear peptides **6** were cleaved from the resin with 1% TFA in CH_2Cl_2 (4 × 5 ml), and the org. fractions were recovered in a flask containing pyridine (250 µl). The org. phases were washed with H_2O (3 × 20 ml), concentrated under reduced pressure, and the resulting residue was dried *in vacuo*. The purity of the linear, protected peptides was checked by HPLC (*Vydac 218TP104*, gradient: 20–100% MeCN/H_2O with 0.1% TFA in 15 min). The protected peptide (200 mg, *ca.* 80 µmol), HATU (91 mg, 0.24 mmol), HOAt (33 mg, 0.24 mmol), and iPr_2NEt (164 µl, 0.96 mmol) in DMF (100 ml) was stirred for 16 h at r.t. The solvent was removed under reduced pressure, and the cyclic peptide was precipitated by addition of H_2O. After centrifugation, the aq. phase was discarded, and the pellet was dried *in vacuo*. The resulting protected cyclic peptide (100 mg, *ca.* 40 µmol) and $[Pd(PPh_3)_4]$ (23 mg, 20 µmol), were dissolved in CH_2Cl_2 (4 ml) (a few drops of DMF were added in case of incomplete dissolution), before $PhSiH_3$ (370 µl, 3 mmol) was added. The mixture was stirred for 1 h at r.t. under N_2. The Alloc-deprotected cyclic peptides **7** were precipitated from the mixture by addition of hexane (30 ml). After centrifugation, the supernatant was discarded, and the pellet was washed with hexane/CH_2Cl_2 6:1 (3 × 20 ml). After drying, the peptide was purified by reversed-phase HPLC (*Vydac 218TP1022*, gradient: 20–100% MeCN/H_2O with 0.1% TFA in 12 min) to afford 25 to 60 mg of pure **7** (25% to 60% yield). The identity of the products was confirmed by ESI-MS.

Coupling to PE-succ-OH and Deprotection. To the cyclic peptide **7** (40 mg, 16 µmol) dissolved in DMF (1 ml) was added a soln. of PE-succ-OH (39 mg, 48 µmol), HATU (18 mg, 48 µmol), HOAt (6 mg, 48 µmol), and iPr_2NEt (27 µl, 0.16 mmol) in DMF (1 ml). This soln. was stirred for 16 h at r.t. The solvent was removed under reduced pressure. H_2O was added to the resulting oily residue. After centrifugation, the supernatant was discarded, the pellet was washed with H_2O (2 × 2 ml) and dried *in vacuo*. The resulting conjugate was then treated with TFA/H_2O/TIPS 95:2.5:2.5 (5 ml) for 2 h at r.t. The mixture was concentrated under reduced pressure, and the residue was dissolved in a H_2O/EtOH mixture. The resulting soln. was washed with $(^iPr)_2O$ (3×) and purified on a C_4 semi-prep. HPLC column (*Vydac 214TP1010*, gradient: 20–100% MeCN/H_2O with 0.1% TFA in 15 min) to afford 3–14 mg of the conjugate **8** (*ca.* 8–37% yield). The purities of the final products, estimated by HPLC, were ≥90% (*Vydac 214TP104*, gradient: 20–100% MeCN/H_2O with 0.1% TFA in 15 min). For ESI-MS, *cf.* the *Table*.

REFERENCES

[1] 'Synthetic peptides as antigens – Ciba Foundation Symposium No. 119', Eds. R. Porter, J. Whelan, John Wiley & Sons, Chichester, UK, 1986.
[2] R. Moreno, L. Jiang, K. Moehle, R. Zurbriggen, R. Glück, J. A. Robinson, G. Pluschke, *ChemBioChem* **2001**, *2*, 838.
[3] C. Bisang, L. Jiang, E. Freund, F. Emery, C. Bauch, H. Matile, G. Pluschke, J. A. Robinson, *J. Am. Chem. Soc.* **1998**, *120*, 7439.
[4] B. Pfeiffer, E. Peduzzi, K. Moehle, R. Zurbriggen, R. Glück, G. Pluschke, J. A. Robinson, *Angew. Chem., Int. Ed.* **2003**, *42*, 2368.
[5] F. Pöltl-Frank, R. Zurbriggen, A. Helg, F. Stuart, J. A. Robinson, R. Glück, G. Pluschke, *Clin. Exp. Immunol.* **1999**, *117*, 496.
[6] O. Nussbaum, M. Lapidot, A. Loyter, *J. Virol.* **1987**, *61*, 2245.
[7] R. Bron, A. Ortiz, J. Dijkstra, T. Stegmann, J. Wilschut, *Meth. Enzymol.* **1993**, *220*, 313.
[8] R. Glück, R. Mischler, B. Finkel, J. U. Que, B. Scarpa, S. J. Cryz, *Lancet* **1994**, *344*, 160.
[9] L. Loutan, P. Bovier, B. Althaus, R. Glück, *Lancet* **1994**, *343*, 322.
[10] T. Triglia, J. Healer, S. R. Caruana, A. N. Hodder, R. F. Anders, B. S. Crabb, A. F. Cowman, *Mol. Microbiol.* **2000**, *38*, 706.
[11] R. F. Anders, P. E. Crewther, S. Edwards, M. Margetts, M. L. Matthew, B. Pollock, D. Pye, *Vaccine* **1998**, *16*, 240.
[12] C. H. M. Kocken, C. Withers-Martinez, M. A. Dubbeld, A. van der Wel, F. Hackett, M. J. Blackman, A. W. Thomas, *Infect. Immun.* **2002**, *70*, 4471.
[13] A. N. Hodder, P. E. Crewther, M. L. S. M. Matthew, G. E. Reid, R. L. Moritz, R. J. Simpson, R. F. Anders, *J. Biol. Chem.* **1996**, *271*, 29446.
[14] M. Nair, M. G. Hinds, A. M. Coley, A. N. Hodder, M. Foley, R. F. Anders, R. S. Norton, *J. Mol. Biol.* **2002**, *322*, 741.
[15] M. S. Mueller, A. Renard, F. Boato, D. Vogel, M. Naegeli, R. Zurbriggen, J. A. Robinson, G. Pluschke, *Infect. Immun.* **2003**, *71*, 4749.
[16] P. D. Sun, D. R. Davies, *Annu. Rev. Biophys. Biomol. Struct.* **1995**, *24*, 269.
[17] J. Murray-Rust, N. Q. McDonald, T. L. Blundell, M. Hosang, C. Oefner, F. Winkler, R. A. Bradshaw, *Structure* **1993**, *1*, 153.
[18] L. Jiang, K. Moehle, B. Dhanapal, D. Obrecht, J. A. Robinson, *Helv. Chim. Acta.* **2000**, *83*, 3097.
[19] M. Favre, K. Moehle, L. Jiang, B. Pfeiffer, J. A. Robinson, *J. Am. Chem. Soc.* **1999**, *121*, 2679.
[20] A. Descours, K. Moehle, A. Renard, J. A. Robinson, *ChemBioChem* **2002**, *3*, 318.
[21] S. C. Shankaramma, Z. Athanassiou, O. Zerbe, K. Moehle, C. Mouton, F. Bernardini, J. W. Vrijbloed, D. Obrecht, J. A. Robinson, *ChemBioChem* **2002**, *3*, 1126.
[22] L. Jiang, M. Favre, K. Moehle, J. A. Robinson, *Chimia* **2000**, *54*, 558.
[23] S. R. Chhabra, B. Hothi, D. J. Evans, P. D. White, B. W. Bycroft, W. C. Chan, Tetrahedron *Lett.* **1998**, *39*, 1603.
[24] B. P. Gangamani, V. A. Kumar, K. N. Ganesh, *Tetrahedron* **1996**, *52*, 15017.
[25] W. C. Chan, P. D. White, in 'The Practical Approach Series', Ed. B. D. Hammes, Oxford University Press, Oxford, 2000.

Received August 30, 2003